European Journal of Pharmacology 904 (2021) 174131

Contents lists available at ScienceDirect

European Journal of Pharmacology

journal homepage: www.elsevier.com/locate/ejphar

Cytotoxicity and apoptosis of nanoparticles on osteosarcoma cells using doxorubicin and methotrexate: A systematic review

Masomeh Maleki [a,b,1], Asal Golchin [c,1], Forough Alemi [d], Simin Younesi [e], Zatollah Asemi [f], Samira Javadi [g], Payam Ali Khiavi [a], Jafar Soleinmapour [h,*], Bahman Yousefi [d,**]

[a] Department of Biochemistry and Clinical Laboratories, Faculty of Medicine, Tabriz University of Medical Sciences, Tabriz, Iran
[b] Student's Research Committee, Tabriz University of Medical Sciences, Tabriz, Iran
[c] Department of Clinical Biochemistry, Faculty of Medicine, Urmia University of Medical Sciences, Urmia, Iran
[d] Drug Applied Research Center, Tabriz University of Medical Sciences, Tabriz, Iran
[e] School of Health and Biomedical Sciences, RMIT University, Melbourne, Vic., Australia
[f] Research Center for Biochemistry and Nutrition in Metabolic Diseases, Kashan University of Medical Sciences, Kashan, Iran
[g] Department of Clinical Biochemistry, School of Medicine, Zanjan University of Medical Sciences, Zanjan, Iran
[h] Department of Orthopedics Surgery, Shohada Teaching Hospital, Tabriz University of Medical Sciences, Tabriz, Iran

ARTICLE INFO

Keywords:
Osteosarcoma
Cytotoxicity
Drug delivery
Nanoparticles
Doxorubicin
Methotrexate

ABSTRACT

The safe development of nanotechnology and usage of nanoparticles (NPs) require the cellular toxicity examination of these NPs. Systematic studies are necessary to collect related data and comparison of the physicochemical features of NPs and their effects on cellular viability on model systems. In the present study, we systematically reviewed original studies, which investigated the cytotoxic effects and apoptosis of free NPs (loaded with doxorubicin (Dox)/or methotrexate (MTX)) via in vitro models. Articles were systematically collected by screening the literature published online in the following databases; PUBMED and SCOPUS and Web of Science and EMBASE. 23 in vitro cytotoxicity studies with 8 apoptosis examinations were found on osteosarcoma (OS) cell lines (mostly on MG-63). 43.47% of the synthesized NPs (10 studies) showed no cytotoxicity to OS cells. 39.13% of the synthesized NPs (9 studies) showed time and/or concentration related-cytotoxicity. Potent cytotoxic synthesized NP did not state. Significance difference between the half-maximal inhibitory concentration (IC50) of drug and drug/NP reported in all studies. Involved NPs in this systematic review for delivery of Dox/or MTX to OS cells have higher safety index and biocompatibility, although small and positively charged NPs acted more toxic in comparison to larger and negative ones, apoptosis rate like cytotoxicity index was notable in drug/NP group, to apply them in clinical works. Future studies are required to address the mechanisms involved in cytotoxicity and apoptosis with a special focus on in vivo investigations.

1. Introduction

Osteosarcoma (OS) is the most common malignant tumor and bone tumor in children and adults. It is the third most common cancer in the world. The annual incidence of osteosarcoma is about 400–1000 new cases in the USA and 2–39 per 2 million people in Europe. OS is estimated to be more common in men than in women, and the three sites of the proximal humerus, proximal tibia, and distal femur are majorly affected by OS(Bielack et al., 2010). Routine OS therapies are chemotherapy and surgery in combination with chemotherapy, which increases the survival rate to 70-60%. Approximately 30% of patients do not respond to treatment due to lung metastasis (the most common site for bone metastasis), recurrence of the disease, side effects, and multidrug resistance (Susa et al., 2009).

Doxorubicin (Dox) and methotrexate (MTX) are two of the most important chemotherapeutic drugs, which are currently used in the treatment of OS. Dox produces formaldehyde that covalently binds DNA and inhibits the function of topoisomerase-II, and finally prevents the synthesis of DNA, RNA, and protein. MTX, as a folic acid antagonist, inhibits the synthesis of protein by inhibiting dihydrofolate reductase

* Corresponding author.
** Corresponding author.
E-mail addresses: soleimanpourj@tbzmed.ac.ir (J. Soleinmapour), yousefib@tbzmed.ac.ir (B. Yousefi).
[1] These authors have contributed equally.

https://doi.org/10.1016/j.ejphar.2021.174131
Received 31 December 2020; Received in revised form 22 April 2021; Accepted 26 April 2021
Available online 30 April 2021

enzyme, which reduces dihydrofolic acid to tetrahydrofolic acid (Gurunathan et al., 2019; Nogueira et al., 2013).

Despite that systemic chemotherapy increases survival in patients with OS, intravenous or oral administration can lead to many side-effects such as ulcerative stomatitis, thrombocytopenia, anemia, cardiotoxicity, liver toxicity, nephrotoxicities, myelosuppression, alopecia (Haghiralsadat et al., 2017; Nayak et al., 2016). The development of biocompatible NPs has promising potential with great importance to prevent the non-specific distribution of drugs in healthy tissues and reduce the side effects of chemotherapy (González-Fernández et al., 2015). Liposomes, micelles, dendrimers, solid lipids, polymer nanoparticles, ceramic nanoparticles, protein nanoparticles, metal nanoparticles, carbon nanotubes, and magnetic nanoparticles are among the nanoparticles available for use in the drug delivery system (Byrne et al., 2008).

The drug delivery system can increase drug permeability, solubility, and half-life in the circulation by inhibiting the reticuloendothelial system. The ability to escape multi-drug resistance, improved pharmacokinetics, and specific drug delivery to target tissues are other benefits of this system that can be pointed (Hu et al., 2010; Wilczewska et al., 2012). The biological and physicochemical properties of nanocarrier cause easier for cells to absorb than larger cells, and by preventing rapid drug degradation, increase the concentration of the drug in the target tissues, where low doses of the drug are required and by preventing the rapid destruction of the drug, it leads to an increase in the concentration of the drug in the target tissues, therefore, requires low doses of the drug (Şahin et al., 2018).

These benefits have made NP a promising candidate in treating cancer patients. In this regard, various in-vitro studies have been conducted to assess the effect of these NPs. In the present systematic review, we summarized the results of studies that assessed cytotoxic effect and apoptosis of free NPs (loaded with Dox/or MTX) via in vitro models.

2. Materials and methods

The systematic review was conducted and reported according to the principles in the Preferred Reporting Items for Systematic Reviews and Meta-Analyses (PRISMA) statement.

2.1. Research questions

The primary research questions of this review were as follows:

- What are the effects of free NPs (loaded with Dox and MTX) on the cytotoxicity of osteosarcoma cancer cells?
- What are the effects of free NPs (loaded with Dox and MTX) on apoptosis in osteosarcoma cancer cells?

2.2. Search strategy

To determine the state-of-the-art related effects of nanoparticles loaded on osteosarcoma cancer, the PUBMED, SCOPUS, Web of Science, and EMBASE were searched. The search strategy for each database is provided in Table 1.

2.3. Inclusion criteria

The scientific papers with the following characteristics were included; (1) papers written in English, (2) published as a full article, (3) articles that have evaluated the rate of cytotoxicity and apoptosis in osteosarcoma cells through reliable methods, (4) articles that have clearly defined and measured outcomes (the half-maximal inhibitory concentration (IC50), cell viability, cell death, and apoptosis), (5) Comparison of Dox and MTX loaded nanoparticles and control groups with free drugs.

Table 1
Search strategy for each database.

SCOPUS 21/9/20	((TITLE-ABS-KEY (methotrexate)) OR (TITLE-ABS KEY (doxorubicin OR farmiblastina OR ribodoxo OR rubex OR adriamycin OR adriblastin* OR adriablastin* OR adrimedac OR doxocell OR doxo AND cell OR doxolem OR doxotec OR myocet OR onkodox))) AND (TITLE-ABS-KEY (osteosarcoma* OR sarcoma* OR osteogenic* OR "bone sarcoma")) AND (TITLE-ABS-KEY (nanoparticle* OR nanocrystals* OR "nanocrystalline materials"))
Pubmed 31/9/20	((((((((((((((((((Doxorubicin[Title/Abstract]) OR Doxorubicin[MeSH Terms]) OR Doxorubicin[Other Term]) OR Farmiblastina[Title/Abstract]) OR Ribodoxo[Title/Abstract]) OR Rubex[Title/Abstract]) OR Adriamycin[Title/Abstract]) OR Adriblastin*[Title/Abstract]) OR Adriablastin*[Title/Abstract]) OR Adrimedac[Title/Abstract]) OR DOXO-cell[Title/Abstract]) OR Doxolem[Title/Abstract]) OR Doxotec[Title/Abstract]) OR Myocet[Title/Abstract]) OR Onkodox [Title/Abstract])) OR (((Methotrexate*[Title/Abstract]) OR Methotrexate[MeSH Terms]) OR Methotrexate*[Other Term]))) AND ((((((nanoparticle*[Title/Abstract]) OR nanoparticle[MeSH Terms]) OR nanoparticle*[Other Term]) OR nanocrystal*[Title/Abstract]) OR Nanocrystal*[Other Term]) OR "nanocrystalline materials"[Title/Abstract]) OR "nanocrystalline materials"[Other Term])) AND ((((((((osteosarcoma*[Title/Abstract]) OR osteosarcoma[MeSH Terms]) OR osteosarcoma*[Other Term]) OR "bone sarcoma"[Title/Abstract]) OR "bone sarcoma"[MeSH Terms]) OR sarcoma *[Title/Abstract]) OR sarcoma *[Other Term]) OR osteogenic*[Title/Abstract]) OR osteogenic*[Other Term])
Embase 31/9/20	**'osteosarcoma'**/exp OR **'osteosarcoma'** OR **'osteosarcoma'**:ab,kw,ti OR **'sarcoma'**/exp OR **'sarcoma'** OR **'sarcoma'**:ab,kw,ti OR **'osteogenic'** OR **'osteogenic'**:ab,kw,ti OR **'bone sarcoma'**/exp OR **'bone sarcoma'** OR **'bone sarcoma'**:ab,kw,ti AND **'nanoparticle'**/exp OR **'nanoparticle'** OR **'nanoparticle'**:ab,kw,ti OR **'nanocrystals'**/exp OR **'nanocrystals'** OR **'nanocrystals'**:ab,kw,ti OR **'nanocrystalline materials'** OR **'nanocrystalline materials'**:ab,kw,ti AND **'methotrexate'**/exp OR **'methotrexate'** OR **'methotrexate'**:ab,kw,ti OR **'doxorubicin'**/exp OR **'doxorubicin'** OR **'doxorubicin'**:ab,kw,ti
Web of science 29/9/20	(TI=(osteosarcoma* OR "bone sarcoma") *AND* DOCUMENT TYPES: (Article) *Indexes=SCI-EXPANDED, SSCI, CPCI-S, CPCI-SSH, ESCI Timespan=All years* (TI= (nanoparticle* OR Nanocrystals* OR Nanocrystalline Materials*) *AND* DOCUMENT TYPES: (Article) *Indexes=SCI-EXPANDED, SSCI, CPCI-S, CPCI-SSH, ESCI Timespan=All years* (TI= (doxorubicin OR farmiblastina OR ribodoxo OR rubex OR adriamycin OR adriblastin* OR adriablastin* OR adrimedac OR doxo-cell OR doxo AND cell OR doxolem OR doxotec OR myocet OR onkodox)) *OR* DOCUMENT TYPES: (Article) *Indexes=SCI-EXPANDED, SSCI, CPCI-S, CPCI-SSH, ESCI Timespan=All years* TI=(methotrexate) *OR* DOCUMENT TYPES: (Article) *Indexes=SCI-EXPANDED, SSCI, CPCI-S, CPCI-SSH, ESCI Timespan=All years*

2.4. Exclusion criteria

The papers with the following characteristics were excluded; (1) review articles, (3) letters to the editor, (4) case reports, (5) editorials.

2.5. Data collection

An author-designed data extraction form was used for data extraction that included first author name, publication year, NP type, NP size (nm), NP morphology, cell line, drug type, exposure assay, exposure time, NP dose, IC50, cell viability, apoptosis rate and necrosis rate.

3. Results

3.1. Characteristics of the included studies

An initial databases search recovered 698 articles, from which, 126 articles were duplicates. Thus 572 articles were assessed for eligibility based on title and abstract from which 527 articles were removed (368 articles were reviews, editorial, conference abstract, short study,

conference paper, observation study, case report, and 142 articles were unrelated). Out of the remaining 62 articles, 39 articles were removed 23 articles were included for the systematic review. The detailed flow chart is provided in Fig. 1. Among remaining articles, 23 in vitro cytotoxicity studies with 8 apoptosis examination found on osteosarcoma cell lines which carried out on MG-63 (9 articles) (Fang et al., 2017; Huang et al., 2020; Iram et al., 2017; Kamba et al., 2013; Li et al., 2017; Prasad et al., 2020; Wei et al., 2019; Yang et al., 2018, 2020), SaOS-2 (7 articles) (Ahmadi et al., 2020; Gu et al., 2019; Huang et al., 2020; Iram et al., 2017; Masoudi et al., 2018; Meshkini and Oveisi, 2017; Sarda et al., 2018; Tapeinos et al., 2018), MNNG-HOS (4 articles) (Fang et al., 2017; Federman et al., 2012; Huang et al., 2020; Oh et al., 2006), hFOB1.19 (3 articles) (Fu et al., 2017; Huang et al., 2020; Steckiewicz et al., 2020), U2OS (2 articles) (Fang et al., 2017; Huang et al., 2020), K7M2 (2 articles) (Li et al., 2020; Nguyen et al., 2016), KHOS(Wang et al., 2016), HOS(Federman et al., 2012), 143B (Steckiewicz et al., 2020), RSaOS-2 (Meshkini and Oveisi, 2017), KHOS-240S (Federman et al., 2012), HOB(Fang et al., 2017),UMR-106 (Fu et al., 2017), Rat primary osteoblast cells (Iram et al., 2017) and patient-derived cell lines (González-Fernández et al., 2017). The maximum number of cell lines used is related to *Huang X*'s (Huang et al., 2020) study carried out with five cell lines. Different cytotoxicity tests applied such as MTT assay (15 articles) (Ahmadi et al., 2020; Fang et al., 2017; Federman et al., 2012; Fu et al., 2017; Iram et al., 2017; Kamba et al., 2013; Li et al., 2017, 2020; Masoudi et al., 2018; Meshkini and Oveisi, 2017; Nguyen et al., 2016; Prasad et al., 2020; Sarda et al., 2018; Steckiewicz et al., 2020; Wang et al., 2016), WST-8 assay (4 articles) (Gu et al., 2019; Huang et al., 2020; Wei et al., 2019; Yang et al., 2018), LDH assay (2 articles) (Kamba et al., 2013; Meshkini and Oveisi, 2017), MTS assay (2 articles) (González-Fernández et al., 2017; Yang et al., 2020), WST-1 assay (Tapeinos et al., 2018), Trypan Blue assay (Oh et al., 2006) and Brdu assay (Kamba et al., 2013). Apoptosis examination studies consist of FITC Annexin-V staining (3 articles) (Fu et al., 2017; Li et al., 2017; Tapeinos et al., 2018), Cell Cycle assay (3 article) (Fu et al., 2017; Meshkini and Oveisi, 2017; Oh et al., 2006), Hoechst 33342 staining (2 articles) (Li et al., 2017; Meshkini and Oveisi, 2017), Caspase-Glo-3/7 (2 article) (González-Fernández et al., 2017; Yang et al., 2020) and PE-Annexin V/7-amino-actinomycin D (7-AAD) (Huang et al., 2020). Based on material used for NPs synthetization, three groups appeared: a) organic nanoparticles such as micelles, liposomes and organic polymers, (47.82% studies with 11 articles) (Fang et al., 2017; Federman et al., 2012; González-Fernández et al., 2017; Gu et al., 2019; Li et al., 2017, 2020; Nguyen et al., 2016; Wang et al., 2016; Wei et al., 2019; Yang et al., 2018, 2020) b) inorganic nanoparticles such as metal and metal oxide NPs (47.82% studies with 11 articles) (Ahmadi et al., 2020; Fu et al., 2017; Iram et al., 2017; Kamba et al., 2013; Masoudi et al., 2018; Meshkini and Oveisi, 2017; Oh et al., 2006; Prasad et al., 2020; Sarda et al., 2018; Steckiewicz et al., 2020; Tapeinos et al., 2018) and c) carbon based NPs such as graphene (4.34% studies with 1 article) (Huang et al., 2020). Morphology report of NPs stated as spherical (69.56% studies with 16 articles) (Ahmadi et al., 2020; Fang et al., 2017; Federman et al., 2012; Fu et al., 2017; Gu et al., 2019; Iram et al., 2017; Li et al., 2017, 2020; Masoudi et al., 2018; Nguyen et al., 2016; Prasad et al., 2020; Steckiewicz et al., 2020; Tapeinos et al., 2018; Wang et al., 2016; Wei et al., 2019; Yang et al., 2020), road shape (8.69% studies with 2 articles) (Kamba et al., 2013; Meshkini and Oveisi, 2017), plate-like (8.69% studies with 2 articles) (Huang et al., 2020; Oh et al., 2006), needle-like (4.34% studies with 1 article) (Sarda et al., 2018) and disk-like (4.34% studies with 1 article) (Yang et al., 2018). One studies reported no morphological data (González-Fernández et al., 2017). Size

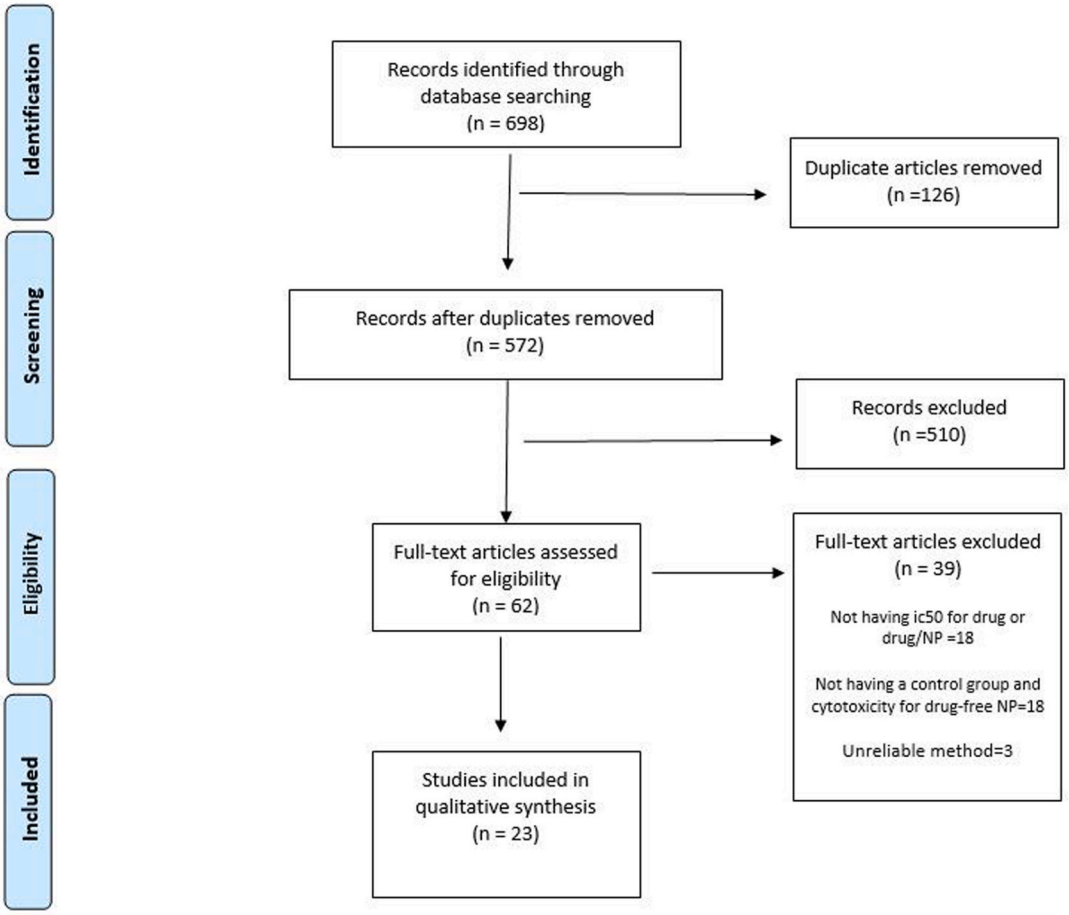

Fig. 1. Flowchart describing the study design process.

distributions of NPs categorized as 5 articles with 1–50 nm (Fang et al., 2017; Fu et al., 2017; Iram et al., 2017; Masoudi et al., 2018; Steckiewicz et al., 2020; Tapeinos et al., 2018), 8 articles with 50–100 nm (González-Fernández et al., 2017; Gu et al., 2019; Iram et al., 2017; Kamba et al., 2013; Li et al., 2020; Nguyen et al., 2016; Sarda et al., 2018; Wang et al., 2016), 6 articles with 100–200 nm (Huang et al., 2020; Li et al., 2017; Meshkini and Oveisi, 2017; Oh et al., 2006; Wei et al., 2019; Yang et al., 2020) and 3 articles with >200 nm (Ahmadi et al., 2020; Prasad et al., 2020; Yang et al., 2018). Dox and MTX were applied in 18 and 6 articles (78.26% and 26.08% studies) respectively. Four articles examined the synergistic effect of Dox with Cisplatin (CIS) (Iram et al., 2017), Edelfosine (González-Fernández et al., 2017; Yang et al., 2020), Curcumin (Wang et al., 2016) and MTX (Prasad et al., 2020). 43.47% of the synthesized NPs (10 studies) showed no cytotoxicity to OS cells. 39.13% of the synthesized NPs (9 studies) showed time and/or concentration related-cytotoxicity to OS cells. Potent cytotoxic synthesized NP did not stated. Four studies did not report free NP cytotoxic data. Significance difference between IC50 of drug and drug/NP reported in all studies. Described methodology including drug and drug/NPs IC50, cell viability of NPs, drug and drug/NPs, duration of exposure, selected cytotoxicity or apoptosis assessment stated in Tables 2 and 3 as cytotoxicity and apoptosis examination (in Vitro) outcomes.

4. Discussion

4.1. Nanotoxicity of NPs

Nanotechnology could improve the current status of medicine by presenting selective therapeutics in the targeted therapy discipline. In this way, it could help us achieve more efficient therapeutics with decreased side effects. Nanoparticles also provide a unique platform for creating multifunctional drug delivery carriers with controlled-release features, in the field of biomedicine. By delivering therapeutic agents to the infected site and increase the accumulation of therapeutic levels at the target site, utilization of NP-based therapies is needed to achieve a less invasive and more selective treatment regime in cancer treatment (Barua and Mitragotri, 2014). Nevertheless, serious and potential dangers from nanoparticle exposure cannot be overlooked, although there are various advantages of nanotechnology applications as mentioned. The toxicity of nanoparticles has been studied in both cell line systems and various organisms, including humans. However, for the safe growth and development of nanotechnology, more examinations about the cellular toxicity of nanoparticles are required. Nanotoxicity introduces the study of the potentially toxic effects of nanoparticles on biological systems. Physicochemical features of NPs and their effects on cellular viability on model systems should be considered, so systematic studies are necessary to collect related data and comparison (Oberdörster, 2010; Shin et al., 2015). Basic in vitro methods used to evaluate the toxicity of NPs has two general classes: viability assays and functional assays. Viability assays are related to death in a cell or a system of cells caused by NPs. Metabolic activity measurement and apoptosis/necrosis assay grouped in viability assays. Considerably, metabolic activity assessments are the typical methods used to detect NPs exposure cell viability. Analyses of the pointers in programmed cell death (i.e., apoptosis) and/or necrosis reveal NPs' direct ability to induce intracellular suicide mechanisms or cell death. Such assays mainly concentrate on measuring membrane integrity, but some also try to measure apoptotic protein levels/activation and DNA fragmentation (Love et al., 2012). This study systematically reviews the toxic potential of NPs and the difference between drug and drug/NPs induced cytotoxicity and apoptosis determined with in vitro assays for osteosarcoma using documented data from a literature review.

4.1.1. In vitro cytotoxicity and apoptosis studies of NPs on OS cells

In the case of non-toxic NPs, the effect of free $CaCO_3$ nanocrystals synthesized from *Kamba SA* on MG 63 cancer cells, even at higher concentrations of 800 to 1000 μg/ml showed a good cytocompatibility of calcium carbonate nanocrystals with no apparent toxicity to MG 63 cells (Kamba et al., 2013). A similar result stated in *Zhenhua Fang*'s study based on nontoxic polymeric micelle self-assembled from Arginyl-glycyl-aspartic acid terminated poly (ethylene glycol)-block-poly (trimethylene carbonate) at a tested concentration up to 1000 μg/ml, indicating superior biocompatibility structures of polymers for both osteosarcoma cells and healthy osteoblast cells (HOB cell line) (Fang et al., 2017). *Jae-Min Oh*'s layered double hydroxide NPs does not influence the cell viability at levels up to 500 μg/ml. Free NPs did not affect the cell cycle at concentrations between 1.5 and 384 μg/ml for 20 h. It's because of their specific internalization pathway via clathrin-mediated cellular uptake (Oh et al., 2006). In *Delshad Ahmadi's* study, the free cationic cyclodextrin coated magnetic NP had cell viability of more than 80% at 400 μg/ml concentration in Saos-2 cells (Ahmadi et al., 2020). Superparamagnetic iron-doped nanocrystalline apatite with SaOs-2 cell line for time intervals of 24, 48, and 72 h showed no significant reduction in cell viability compared to the control (Sarda et al., 2018). The same non-toxic results of NPs are stated in studies (Huang et al., 2020; Li et al., 2017; Sarda et al., 2018; Wang et al., 2016). Metabolic activity of CeO_2 NPs (Tapeinos et al., 2018) with pH-responsive properties (pH 7.4 and 6) tested on SAOS-2 cell line does not affect the proliferation of the treated cell line. CeO_2 NPs at pH 6.0 did not generate reactive oxygen species leading to reactive oxygen species -mediated apoptosis and a reduction in the proliferation of SAOS-2. 100% cell viability for CeO_2 NPs in 50 μg/m (120 h) at pH 7.4 and 6 reported. It is because of the antioxidant properties of CeO2 NPs increased cell number due to high proliferation and the increased reactive oxygen species scavenging by SAOS-2 cells reported in this study. A pH value around 6 enhances the cytotoxicity of CeO_2 NPs and increases cell death. In second pH-responsive NP, mesoporous zeolites/chitosan core-shell nanodisks (Yang et al., 2018) showed ~95% cell viability in pH 7.4, 6 and 5.5 on the MG63 cells. This result showed the high biocompatibility of this NP.

Several studies reported the nanotoxicity of synthesized NPs in a time and/or concentration manner. In synthesized cockle shells-derived aragonite NPs by *Wenliang Fu,* viability percentage was higher than 80%, at a high concentration of 500 mg/ml because of the gravity sedimentation. These NPs precipitated and covered the cell surface, which would block the cells to get enough nutrients and oxygen from the culture medium. Thus, when the cells were exposed to 500–1000 μg/ml concentrations, the cell viability was decreased and concentration related-cytotoxicity stated 70% and 75% cell viability at 1000 μg/ml, on UMR-106 and hFOB 1.19 cell lines reported. Additionally, no significant difference between the free NPs group and the control group reported in apoptosis and cell cycle arrest rate on UMR-106 cells even at 72 h, therefore good biocompatibility presented by this NP(Fu et al., 2017). Fluorescent titania NPs synthesized from *Mina Masoudi* had low cytotoxicity at 50 μg/ml on SaOs-2 cells. IC50 value stated 125 μg/ml for this NP. The study highlighted their cytotoxicity of synthesized NP is related to oxidative stress by the production of reactive oxygen species (Masoudi et al., 2018). Bromelain gold NP at 0–1 μg/ml led to dose-dependent cytotoxicity against MG-63 and Saos-2 cells and showed no significant toxicity at the given concentration. The use of bromelain as a reducing agent and capping agent to synthesize gold NPs reduced strongly auric chloride and formed stable corona on the surface of gold NPs (Iram et al., 2017). At 100 μg/ml of *Tuyen Duong Thanh Nguyen* prepared alendronic acid-modified lipid and poly lactic-co-glycolic acid (PLGA) polymeric core NPs ~90% cell viability on K7M2 cells reported and when this concentration rises to 150 ug/ml, cell viability decreases to 80%, this reflection clarified by masking of the cellular surface under 96-well plate environment, hence reduce the cellular accessibility to oxygen and creating a negative growing environment to the cell which further induces unforeseen cell death (Nguyen et al., 2016). No cytotoxicity was found under 100 μg/ml for isolated exosomes from bone

Table 2
The cytotoxic properties of synthesized nanosystems on OS cells (in vitro).

Type	Size	Zeta Potential (Mv)	Drug	Exposure Time	Drug Ic50	Drug/NP Ic50	Drug Cell Viability	Drug/NP Cell Viability	NP Cell Viability	Ref.
Bromelain gold NP	9.2 nm	−19.5	CIS and Dox	48 h	0.144 (DoxX/MG-63) 0.177 (Dox/saos-2)	0.07 μg/ml (MG-63). 0.09 μg/ml (Saos-2).	~70% (cis) ~30% (Dox) in 0.5 μg/ml	MG-63, Saos-2: ~10% (with cis and Dox) in 0.5 μg/ml primary osteoblasts cells: ~77% in 1 μg/ml	~95% in 1 μg/ml (MG-63, Saos-2)	Iram et al. (2017)
$CaCO_3$ nanocrystal	100 nm	NA	Dox	24,48 and 72	0.5 μg/ml (48 h)	0.23 μg/ml (24 h)	~27% (24 h) in 2 μg/ml	~23% (24 h) in 2 μg/ml	95% at 1000 μg/ml)	Kamba et al. (2013)
Poloxamer-modified trimethyl chitosan	160 nm	+20.1	MTX	24	4.86 μg/ml	1.92 μg/ml	~30% at 10 μg/ml	~10% at 10 μg/ml	More than 90% at 200 μg/ml	Li et al. (2017)
Fluorescent titania NP	<30 nm	−10.01	Dox	24	0.829 μg/ml	0.283 μg/ml	~60% at 0.5 μg/ml	~40% at 0.5 μg/ml	~55% at 125 μg/ml	Masoudi et al. (2018)
Edelfosine lipid NP	74.7 ± 3.05 nm	−28.4 ± 4.8	Dox	72 h	U-2 OS: 56.33 nM, 595M early passages: 55.50 nM 595M late passages: 255.00 nM	U-2 OS: 47.00 nM, 595M early passages:109.00 nM, 595M late passages: 107.33 nM	NA	NA	90%	González-Fernández et al. (2017)
Arginyl-glycyl-aspartic acid (ethylene glycol)-blockpoly (trimethylene carbonate) micelle	46–73 nm	NA	Dox	48 h	MG-63: 9.72 μg/ml, MNNG-HOS5.78 μg/ml	MG-63: 1.79 μg/ml, MNNG-HOS: 1.42 μg/ml	MG-63: ~30% at 10 μg/ml, MNNG-HOS: ~20% at 10 μg/ml	MG-63: 50% at 10 μg/ml, MNNG-HOS: 40% at 10 μg/ml	MG-63: ~90% in 1000 μg/ml, HOB: ~100% in 1000 μg/ml	Fang et al. (2017)
Anti-Alcam Cell Surface Receptor-hybrid polymerized liposomal NP	NA	NA	Dox	72 h	KHOS 240S: 0.1 μM, HOS: 0.3 μM MNNG-HOS: 2 μM	KHOS 240S: 0.55 μM, HOS: 0.9 μM, MNNG-HOS: 8.5 μM	NA	NA	NA	Federman et al. (2012)
Aragonite NP	20–60 nm	−46.17 ± 3.8	Dox	24,48 and 72 h	UMR-106: ~1 μg/ml in 24 h	UMR-106: 0.202 μg/ml in 72 h	UMR-106: ~7% at 2 μg/ml in 72 h	UMR-106: ~5% at 2 μg/ml in 72 h	UMR-106: 70% at 1000 μg/ml, hFOB 1.19: 75% at 1000 μg/ml	Fu et al. (2017)
Type	**Size**	**Zeta Potential (Mv)**	**Drug**	**Exposure Time**	**Drug Ic50**	**Drug/NP Ic50**	**Drug Cell Viability**	**Drug/NP Cell Viability**	**NP Cell Viability**	**Ref.**
Cerium dioxide NP	0.75 ± 0.25 μm (mean value of 100 particles)	−20.90 ± 2.12	Dox	24,72 and 120	3 μg/ml in 24 h and pH 7.4 <0.5 μg/ml in 24 h and pH 6.	(In 50 μg/ml NP 24 h) ~1 μg/ml in pH 7.4. ~0.5 μg/ml in pH 6.	~17% in 0.6 μg/ml (120 h) pH 7.4. ~15% in 0.6 μg/ml (120 h) pH 6.	~25% in 0.6 μg/ml (120 h) pH 7.4. ~20% in 0.6 μg/ml (120 h) pH 6.	100% in 50 μg/ml (120 h) pH 7.4. 100% in 50 μg/ml (120 h) pH 6.	Tapeinos et al. (2018)
Mesoporous chitosan nanodisks	300 nm diameter and 100 thickness	–	Dox	24 h	10 μg/ml	~7 μg/ml	~50% in 10 μg/ml	~75% in pH 7.5 ~65% in pH 6 ~60% in pH 5.5	~95% in pH 7.4,6,5.5	Yang et al. (2018)
Lipid NP	96.7 ± 2.6 nm	−31.9 ± 3.4	Dox/ Curcumin	24 h	Dox: 46.5 ± 3.1 μM Curcumin: 49.3 ± 3.9	0.6 ± 0.1 μM (Dox + Curcumin)	Dox: ~45% in 50 μM Curcumin: ~45% in 50 μM	~5% in 50 μM (Dox + Curcumin)	~90% in 50 μM	Wang et al. (2016)
Superparamagnetic iron-doped nanocrystalline apatite	10-30 (wide) 70-100 (long) nm	−18 ± 1	MTX	24,48 and 72 h	50 μM (72 h)	~50 μM (72 h)	~45% (72 h) in 5 μM	~35% (72 h) 50 μM	~95% (72 h)	Sarda et al. (2018)
F127@Zn-Hydroxyapatite NP	75.49 (width) 29.24	−26.2	MTX	72 h	Saos-2: 20 μg/ml RSaos-2/	Saos-2: 0.5 μg/ml MTX resistant Saos-2: 60 μg/ml	Saos-2: ~35% in 30 μg/ml MTX	Saos-2: ~18% in 30 μg/ml MTX resistant	Saos-2: ~50% in 10 μg/ml MTX	Meshkini and Oveisi (2017)

(*continued on next page*)

Table 2 (*continued*)

Type	Size	Zeta Potential (Mv)	Drug	Exposure Time	Drug Ic50	Drug/NP Ic50	Drug Cell Viability	Drug/NP Cell Viability	NP Cell Viability	Ref.
	(Length) nm				MTX: 120 μg/ml		resistant Saos-2: ~38% in 180 μg/ml	Saos-2: ~20% in 180 μg/ml	resistant Saos-2: ~30% in 210 μg/ml	
Alendronic acid-modified lipid and PLGA polymeric core NP	69 ± 5 nm	−37.7 ± 2	Dox	24, 48, and 72 h	2.621 μM (48 h)	3.064 μM(48 h)	~18% (48 h) In 5 μM	~18% (48 h) In 5 μM	~70% in 200 μg/ml	Nguyen et al. (2016)
Layered double hydroxide NP	136 ± 29 nm	+20	MTX	72	9 μg/ml	5 μg/ml	~30% in 120 μg/ml	~12% in 110 μg/ml	~100% in 800 μg/ml	Oh et al. (2006)
Type	**Size**	**Zeta Potential (Mv)**	**Drug**	**Exposure Time**	**Drug Ic50**	**Drug/NP Ic50**	**Drug Cell Viability**	**Drug/NP Cell Viability**	**NP Cell Viability**	**Ref.**
MutT homolog 1 inhibitor graphene oxide NP	~160 nm	−19.3	Dox	NA	7 μg/ml	3 μg/ml	40% In 10 μg/ml	20% In 10 μg/ml	90% In 10 μg/ml	Huang et al. (2020)
lipid–polymer hybrid NP	122.5 ± 2.45 nm	−18.4 ± 1.26	Dox	24 h	4.5 μg/ml	1.08 μg/ml	30% In 10 μg/ml	5% In 10 μg/ml	40% In 10 μg/ml	Yang et al. (2020)
Glutathione stabilized Gold NP	2.1 ± 0.3 nm	NA	Dox	24 h	>0.99 μg/ml	143B: > 100 μg/ml	20% In 4.93 μg/ml	70% In 100 μg/ml	65% In 100 μg/ml	Steckiewicz et al. (2020)
Cationic cyclodextrin coated magnetic NP	687.8 ± 17.4 nm	−9.3	MTX	48 h	7.82 μg/ml in 48 h	7.22 μg/ml in 48 h	35% In 40 μg/ml	35% In 40 μg/ml	85% In 400 μg/ml	Ahmadi et al. (2020)
Calcium-mineralized polypeptide NP	124.4 ± 7.9 nm	NA	Dox	48 h	0.25 μg/ml	0.15 μg/ml	~30% In 1.25 μg/ml	~15% In 1.25 μg/ml	NA	Li et al. (2020)
Bovine serum albumin-iridium oxide NP	62 ± 3.2 nm	−30.4	Dox	24 h	19.24 μg/ml	6.21 μg/ml	40% In 100 μg/ml	5% In 100 μg/ml	35% In 100 μg/ml	Gu et al. (2019)
Core shell NP	212 ± 41 nm	NA	Dox/MTX	24, 72 h	Dox: 2.8 μg/ml MTX: 11.5 μg/ml (24 h)	1 μg/ml in 72 h	15% in 2.8 μg/ml Dox and 11.5 μg/ml MTX (72 h)	45% In 100 μg/ml NP and 2.8 μg/ml Dox and 11.5 μg/ml MTX (72 h)	NA	Prasad et al. (2020)
Exosome	112.4 nm	NA	Dox	24 h	10.13 μg/ml	6.48 μg/ml	5% In 100 μg/ml	5% In 100 μg/ml	90%% In 200 μg/ml	Wei et al. (2019)

*NA: Not Available.

marrow mesenchymal stem cells, however 10% cytotoxicity was observed at 200 μg/ml (Wei et al., 2019). The IC50 value of mesoporous zinc hydroxyapatite/F127 stated 10 μg/ml and 110 μg/ml on primary cells (Saos-2) and the MTX-resistant human osteosarcoma Saos-2 cell line respectively. Inhibition of the P-gp pumps by pluronic F127, modulation of the signaling pathways by a raised zinc content leads to more cell death (Meshkini and Oveisi, 2017). Same time and/or concentration cytotoxicity stated in studies (Gu et al., 2019; Steckiewicz et al., 2020; Yang et al., 2020).

5. Impact of physiochemical properties on NPs induced cytotoxicity

The induction of cytotoxicity by NPs is associated with the interaction of NP surface and cellular components. The surface area of the NP increases exponentially as the diameter lessens. NPs can have remarkably various levels of cytotoxicity depending on both particle size and surface reactivity despite NPs have the same structure. Very small NPs have numerous surface curvature to perform required conformational rigidity to enable multivalent binding with receptors. In the case of larger NPs, there is a limit in the process of membrane wrapping for NP internalization. Larger NPs cannot compensate for the depletion of receptors within the binding area through the global diffusive motion of distant receptors (Leroueil et al., 2007; Shin et al., 2015).

Except for NPs size impact on cytotoxicity, effective cellular internationalization depends upon biocompatibility. Also, electronic status is critical to cellular uptake and involved in cytotoxicity.

5.1. Assessing internalization and size-based cytotoxicity of NPs

The size of synthesized NPs that showed cytotoxicity ranged from 29 to 160 nm with defined IC50 at 24 h exposure in vitro showed in Fig. 2. 50% of NPs were from the organic group and 50% from the inorganic group. It was found that the cellular toxicity of NPs exhibited a dependence on particle size. Smaller sized NPs were toxic compared to larger sizes. Numerous studies have revealed the impact of size on NP's cytotoxicity such as *Yu Pan's* (Pan et al., 2007) and *AR Gliga*'s (Gliga et al., 2014) study stated that smaller NPs have smaller IC50 values.

5.2. Assessing surface electrostatic status related cytotoxicity of NPs

The zeta potential of synthesized NPs that showed cytotoxicity ranged from −46.17 ± 3.8 mV to +20.1 with defined IC50 at 24 h exposure in vitro showed in Fig. 3. 44.4% of NPs were from the organic group, 44.4% from the inorganic group, and 1 case from the carbon-based group. NPs with a near-zero or positively charged surface tended to have higher toxicity. This finding is in agreement with several studies, which showed surface charge plays an important role in the

Table 3
The apoptosis rate of synthesized NPs on OS cells (in vitro).

Type	Size (Nm)	Zeta Potential (Mv)	Drug	Exposure Time (Hour)	Apoptosis (Drug/Np)	Necrosis (Drug/Np)	Apoptosis (Free Drug)	Necrosis (Free Drug)	Ref.
Poloxamer modified trimethyl chitosan	160	+20.1	MTX	24	~48% (FITC Annexin V) ~67% (Hoechst 33342)	NA	~25% (FITC Annexin V) ~31% (Hoechst 33342)	NA	Li et al. (2017)
Edelfosine lipid NP	74.7 ± 3.05	−28.4 ± 4.8	Dox/ Edelfosine	48,72	~6 fold increase vs control in 72 h.	NA	~3 fold increase vs control in 72 h.	NA	González-Fernández et al. (2017)
Aragonite NP	20–60	−46.17 ± 3.8	Dox	24, 48 and 72	96.63% (24 h) 99.85% (48 h) 90.13% (72 h) G2/M phase: 45.07 ± 1.43% sub G0/G1 phase 19.27 ± 0.48%	NA	~20% (24 h) ~50% (48 h) ~80% (72 h) G2/M phase: 39.73 ± 1.78% sub G0/G1 phase: 27.94 ± 0.12%.	NA	Fu et al. (2017)
Cerium dioxide NP	100	−20.90 ± 2.12	Dox	24, 72, 120	~0% in 50 μg/ml (120 h) pH 7.4. ~5% in 50 μg/ml (120 h) pH 6.	~75% in 50 μg/ml (24 h) pH 7.4.~90% in 50 μg/ml (24 h) pH 6.	0% in 0.5 μg/ml (24 h) pH 7.4. ~5% in 0.5 μg/ml (24 h) pH 6.	60% in 0.5 μg/ml (24 h) pH 7.4,~95% in 0.5 μg/ml (24 h) pH 6.	Tapeinos et al. (2018)
F127@Zn-Hydroxyapatite NP	75.49 (width) 29.24 (Length)	−26.2	MTX	24,48,72	Saos-2: 43.6% MTX resistant Saos-2: 31.5%	NA	Saos-2: 23.2% MTX resistant Saos-2: 18.8%	NA	Meshkini and Oveisi (2017)
Layered double hydroxide NP	136 ± 29	+20	MTX	20	G1 phase arrest: 77.09%	NA	G1 phase arrest: 63.87%	NA	Oh et al. (2006)
MutT homolog 1 inhibitor graphene oxide NP	~160	−19.3	Dox	NA	24.52%	1.80%	10.64%	0.29	Huang et al. (2020)
Lipid–polymer hybrid NP	122.5 ± 2.45	−18.4 ± 1.26	Dox/ Edelfosine	24	~3.5 fold increase vs Dox.	NA	~1.5 fold increase vs control.	NA	Yang et al. (2020)

*NA: Not Available.

cellular toxicity of NPs, and positively charged NPs were toxic to most of the cancer and normal cell lines studied (Asati et al., 2010; Gratton et al., 2008).

6. Nanoparticle-loaded chemotherapeutic drugs

In the case of encapsulated Dox with $CaCO_3$ were evaluated on the MG 63 OS cell line observed that the cell inhibition rate is dependent on the increase in concentration and incubation periods and CaCO3/Dox was found to be more sensitive than free Dox (Kamba et al., 2013). This resulted in the increase of drug uptake to tumor cells with increased toxicity (Dox IC50 reported in 48 h but CaCO3/Dox IC50 reported in 24 h). Similar findings were observed with fluorescent titania NP delivering Dox, and free Dox. The rapid and effective internalization of Dox/-fluorescent titania NP into cancer cells and also non-covalently bonding of Dox with fluorescent titania NP reported. The drug-loading mode meaning non-covalent complexation or covalent conjugation was also reported as a critical factor that affects therapeutic efficiency so that the non-covalently loaded Dox to NPs displayed significantly higher cytotoxicity than covalently conjugated Dox (Masoudi et al., 2018). Lipid-based nanocarriers such as lipid NPs were also used to deliver Dox (González-Fernández et al., 2017). When the cytotoxic activity of Dox was studied in cells with different passage numbers, the activity of Dox-LN was not influenced by the passage number and they were 2.4 times more effective than free Dox for preventing the growth of high passage metastatic cells, which indicates that NPs may overcome some of the intrinsic resistance mechanisms acquired by metastatic tumor

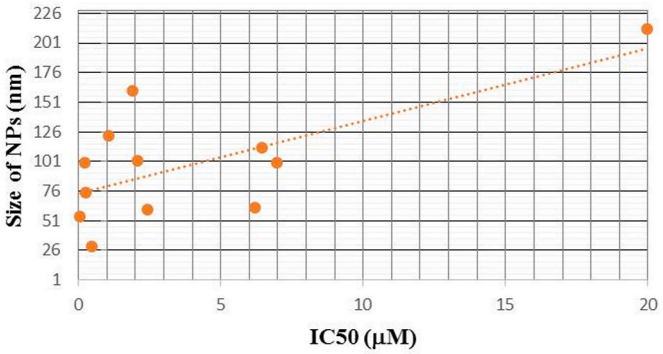

Fig. 2. Correlation between the size of NPs and cytotoxic response at 24 h of exposure in vitro. Correlation between the size of NPs and cytotoxic response at 24 h of exposure. Figure show that cytotoxicity is in reverse related to size; smaller nanoparticles have smaller IC50 values, which explains stronger cytotoxicity. ● Nanoparticles and ------ Trend line.

cells in late stages. This strategy enhanced drug delivery percentage. Formulations of Dox in Arginyl-Glycyl-Aspartic acid poly (ethylene glycol)-block-poly (trimethylene carbonate) micelle (Fang et al., 2017), Anti-Alcam Cell Surface Receptor-hybrid polymerized liposomal NP (Federman et al., 2012), Aragonite NP (Fu et al., 2017), Cerium dioxide NP (Tapeinos et al., 2018), Mesoporous zeolites/chitosan nanodisk (Yang et al., 2018), Alendronic acid-modified lipid and PLGA polymeric

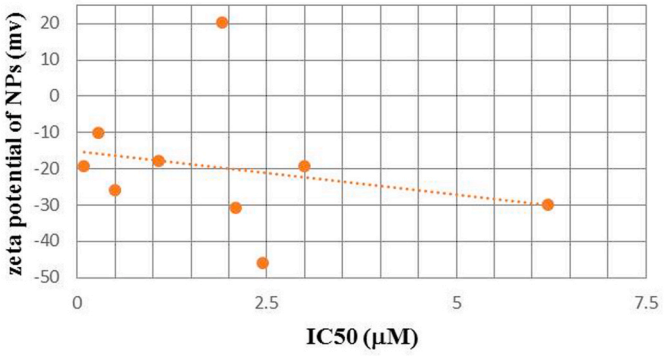

Fig. 3. Correlation between the zeta potential of NPs and cytotoxic response at 24 h of exposure in vitro. Figure show that NPs with a near-zero or positively charged surface tended to have higher toxicity. ● Nanoparticles and ------ Trend line.

core NP (Nguyen et al., 2016), MutT homolog 1 inhibitor graphene oxide NP (Huang et al., 2020), Lipid–polymer hybrid NP (Yang et al., 2020), Glutathione stabilized Gold NP (Steckiewicz et al., 2020), Calcium-mineralized polypeptide NP (Ahmadi et al., 2020), Bovine serum albumin-iridium oxide NP (Gu et al., 2019) and Exosome (Wei et al., 2019) even with different internalization method reported same results in enhancement of drug delivery and the efficacy of the treatment of osteosarcoma.

In the case of MTX encapsulations, a poloxamer surface-modified trimethyl chitosan NP formulation of MTX was reported as a dose-dependent cytotoxic effect in OS cells and anticancer effect compared to that of free MTX. The enhanced cellular uptake of this NP resulted in increased accumulation of MTX in cancer cells that might induce greater cytotoxicity and apoptosis effect (Li et al., 2017). Improvement in the delivery profile of MTX was reported because MTX could penetrate the tumor cell membrane without any early decomposition through a nanostructure-mediated internalization with nanocrystalline apatites (Sarda et al., 2018). The NP substantially increased the cytotoxicity of MTX in mesoporous zinc-substituted hydroxyapatite NP with inhibition of the P-gp pumps by pluronic block copolymer F127, modulation of the signaling pathways by a raised zinc content, and MTX accumulation directed the cells toward death through apoptosis (Meshkini and Oveisi, 2017). Different NPs were shown to improve cytotoxicity and apoptosis (Ahmadi et al., 2020; Oh et al., 2006).

7. Conclusion

This systematic review provides a comparison among the studies and more comprehensive data on delivery of Dox/or MTX to tumors with carriers that are necessary because this strategy will omit a lack of specificity and selectivity and prevent the use of high dosages in the treatment (Patil et al., 2012; Zhang et al., 2020). Moreover, a better conclusion of the overall view of the nanocarrier's cytotoxicity and apoptosis rate can be achieved from this review. The studies analyzed in this review included cytotoxicity and apoptosis assays of NPs and Dox/or MTX-NPs using different OS cell lines, exposure time, size and zeta potential of NPs by using in vitro models. Also, an overview of IC50 in drug and drug/NP groups presented. This variety made it complicated to perform clear comparisons among the available studies. Also laboratory studies on the cytotoxicity and apoptosis potential of synthesized nanocarriers for OS studies are still limited. However collected and presented data suggesting that non-toxic synthesized NPs; $CaCO_3$ nanocrystals, polymeric micelles, layered double hydroxide NPs, magnetic NPs, superparamagnetic iron-doped nanocrystalline, CeO_2 NPs, lipid NPs, poloxamer-modified chitosan, and graphene oxide NPs showed a good cytocompatibility with no apparent toxicity at tested concentrations identified in this review as acceptable test subjects before proceeding to animal studies clinical trials. Analyzing the size and zeta potential of the synthesized nanocarriers is important because it will provide the precise design of nanocarriers with correct and exact sizes and surface charges for the highest accumulation in the tumor site. Involved NPs in this systematic review for delivery of Dox/or MTX to OS cells have higher biocompatibility, although small and positively charged NPs acted more toxic in comparison to larger and negative ones, apoptosis rate like cytotoxicity index was notable in drug/NP group, to apply them in clinical works. Further studies are required to address the mechanisms of cytotoxicity and apoptosis, with a special need for in vivo studies.

Acknowledgements

The Authors would like to thanks Clinical Research Development Unit, Shohada Hospital, Tabriz University of Medical Sciences for kind supports.

References

Ahmadi, D., Zarei, M., Rahimi, M., Khazaie, M., Asemi, Z., Mir, S.M., Sadeghpour, A., Karimian, A., Alemi, F., Rahmati-Yamchi, M., 2020. Preparation and in-vitro evaluation of pH-responsive cationic cyclodextrin coated magnetic nanoparticles for delivery of methotrexate to the Saos-2 bone cancer cells. J. Drug Deliv. Sci. Technol. 101584.

Asati, A., Santra, S., Kaittanis, C., Perez, J.M., 2010. Surface-charge-dependent cell localization and cytotoxicity of cerium oxide nanoparticles. ACS Nano 4, 5321–5331.

Barua, S., Mitragotri, S., 2014. Challenges associated with penetration of nanoparticles across cell and tissue barriers: a review of current status and future prospects. Nano Today 9, 223–243.

Bielack, S., Jürgens, H., Jundt, G., Kevric, M., Kühne, T., Reichardt, P., Zoubek, A., Werner, M., Winkelmann, W., Kotz, R., 2010. Osteosarcoma: the COSS experience. In: Jaffe, N., Bruland, O.S., Bielack, S. (Eds.), Pediatric and Adolescent Osteosarcoma. Springer US, Boston, MA, pp. 289–308.

Byrne, J.D., Betancourt, T., Brannon-Peppas, L., 2008. Active targeting schemes for nanoparticle systems in cancer therapeutics. Adv. Drug Deliv. Rev. 60, 1615–1626.

Fang, Z., Sun, Y., Xiao, H., Li, P., Liu, M., Ding, F., Kan, W., Miao, R., 2017. Targeted osteosarcoma chemotherapy using RGD peptide-installed doxorubicin-loaded biodegradable polymeric micelle. Biomed. Pharmacother. 85, 160–168.

Federman, N., Chan, J., Nagy, J.O., Landaw, E.M., McCabe, K., Wu, A.M., Triche, T., Kang, H., Liu, B., Marks, J.D., 2012. Enhanced growth inhibition of osteosarcoma by cytotoxic polymerized liposomal nanoparticles targeting the alcam cell surface receptor. Sarcoma 2012.

Fu, W., Mohd Noor, M.H., Yusof, L.M., Ibrahim, T.A.T., Keong, Y.S., Jaji, A.Z., Zakaria, M.Z.A.B., 2017. In vitro evaluation of a novel pH sensitive drug delivery system based cockle shell-derived aragonite nanoparticles against osteosarcoma. J. Exp. Nanosci. 12, 166–187.

Gliga, A.R., Skoglund, S., Wallinder, I.O., Fadeel, B., Karlsson, H.L., 2014. Size-dependent cytotoxicity of silver nanoparticles in human lung cells: the role of cellular uptake, agglomeration and Ag release. Part. Fibre Toxicol. 11, 1–17.

González-Fernández, Y., Imbuluzqueta, E., Zalacain, M., Mollinedo, F., Patiño-García, A., Blanco-Prieto, M.J., 2017. Doxorubicin and edelfosine lipid nanoparticles are effective acting synergistically against drug-resistant osteosarcoma cancer cells. Canc. Lett. 388, 262–268.

González-Fernández, Y., Zalacain, M., Imbuluzqueta, E., Sierrasesumaga, L., Patiño-García, A., Blanco-Prieto, M.J., 2015. Lipid nanoparticles enhance the efficacy of chemotherapy in primary and metastatic human osteosarcoma cells. J. Drug Deliv. Sci. Technol. 30, 435–442.

Gratton, S.E., Ropp, P.A., Pohlhaus, P.D., Luft, J.C., Madden, V.J., Napier, M.E., DeSimone, J.M., 2008. The effect of particle design on cellular internalization pathways. Proc. Natl. Acad. Sci. Unit. States Am. 105, 11613–11618.

Gu, W., Zhang, T., Gao, J., Wang, Y., Li, D., Zhao, Z., Jiang, B., Dong, Z., Liu, H., 2019. Albumin-bioinspired iridium oxide nanoplatform with high photothermal conversion efficiency for synergistic chemo-photothermal of osteosarcoma. Drug Deliv. 26, 918–927.

Gurunathan, S., Jeyaraj, M., Kang, M.-H., Kim, J.-H., 2019. Tangeretin-assisted platinum nanoparticles enhance the apoptotic properties of doxorubicin: combination therapy for osteosarcoma treatment. Nanomaterials 9, 1089.

Haghiralsadat, F., Amoabediny, G., Sheikhha, M.H., Forouzanfar, T., Helder, M.N., Zandieh-doulabi, B., 2017. A novel approach on drug delivery: investigation of a new nano-formulation of liposomal doxorubicin and biological evaluation of entrapped doxorubicin on various osteosarcoma cell lines. Cell J. (Yakhteh) 19, 55.

Hu, C.-M.J., Aryal, S., Zhang, L., 2010. Nanoparticle-assisted combination therapies for effective cancer treatment. Ther. Deliv. 1, 323–334.

Huang, X., Chen, J., Wu, W., Yang, W., Zhong, B., Qing, X., Shao, Z., 2020. Delivery of MutT homolog 1 inhibitor by functionalized graphene oxide nanoparticles for enhanced chemo-photodynamic therapy triggers cell death in osteosarcoma. Acta Biomater. 109, 229–243.

Iram, S., Zahera, M., Khan, S., Khan, I., Syed, A., Ansary, A.A., Ameen, F., Shair, O.H., Khan, M.S., 2017. Gold nanoconjugates reinforce the potency of conjugated cisplatin and doxorubicin. Colloids Surf. B Biointerfaces 160, 254–264.
Kamba, S.A., Ismail, M., Hussein-Al-Ali, S.H., Ibrahim, T.A.T., Zakaria, Z.A.B., 2013. In vitro delivery and controlled release of doxorubicin for targeting osteosarcoma bone cancer. Molecules 18, 10580–10598.
Leroueil, P.R., Hong, S., Mecke, A., Baker Jr., J.R., Orr, B.G., Banaszak Holl, M.M., 2007. Nanoparticle interaction with biological membranes: does nanotechnology present a Janus face? Accounts Chem. Res. 40, 335–342.
Li, K., Li, D., Zhao, L., Chang, Y., Zhang, Y., Cui, Y., Zhang, Z., 2020. Calcium-mineralized polypeptide nanoparticle for intracellular drug delivery in osteosarcoma chemotherapy. Bioact. Mater. 5, 721–731.
Li, S., Xiong, Y., Zhang, X., 2017. Poloxamer surface modified trimethyl chitosan nanoparticles for the effective delivery of methotrexate in osteosarcoma. Biomed. Pharmacother. 90, 872–879.
Love, S.A., Maurer-Jones, M.A., Thompson, J.W., Lin, Y.-S., Haynes, C.L., 2012. Assessing nanoparticle toxicity. Annu. Rev. Anal. Chem. 5, 181–205.
Masoudi, M., Mashreghi, M., Goharshadi, E., Meshkini, A., 2018. Multifunctional fluorescent titania nanoparticles: green preparation and applications as antibacterial and cancer theranostic agents. Artif. Cell. Nanomed. Biotechnol. 46, 248–259.
Meshkini, A., Oveisi, H., 2017. Methotrexate-F127 conjugated mesoporous zinc hydroxyapatite as an efficient drug delivery system for overcoming chemotherapy resistance in osteosarcoma cells. Colloids Surf. B Biointerfaces 158, 319–330.
Nayak, D., Ashe, S., Rauta, P.R., Kumari, M., Nayak, B., 2016. Bark extract mediated green synthesis of silver nanoparticles: evaluation of antimicrobial activity and antiproliferative response against osteosarcoma. Mater. Sci. Eng. C 58, 44–52.
Nguyen, T.D.T., Pitchaimani, A., Aryal, S., 2016. Engineered nanomedicine with alendronic acid corona improves targeting to osteosarcoma. Sci. Rep. 6, 36707.
Nogueira, D.R., Tavano, L., Mitjans, M., Pérez, L., Infante, M.R., Vinardell, M.P., 2013. In vitro antitumor activity of methotrexate via pH-sensitive chitosan nanoparticles. Biomaterials 34, 2758–2772.
Oberdörster, G., 2010. Safety assessment for nanotechnology and nanomedicine: concepts of nanotoxicology. J. Intern. Med. 267, 89–105.
Oh, J.-M., Choi, S.-J., Kim, S.-T., Choy, J.-H., 2006. Cellular uptake mechanism of an inorganic nanovehicle and its drug conjugates: enhanced efficacy due to clathrin-mediated endocytosis. Bioconjugate Chem. 17, 1411–1417.
Pan, Y., Neuss, S., Leifert, A., Fischler, M., Wen, F., Simon, U., Schmid, G., Brandau, W., Jahnen-Dechent, W., 2007. Size-dependent cytotoxicity of gold nanoparticles. Small 3, 1941–1949.
Patil, R., Portilla-Arias, J., Ding, H., Konda, B., Rekechenetskiy, A., Inoue, S., Black, K.L., Holler, E., Ljubimova, J.Y., 2012. Cellular delivery of doxorubicin via pH-controlled hydrazone linkage using multifunctional nano vehicle based on poly (β-L-malic acid). Int. J. Mol. Sci. 13, 11681–11693.
Prasad, S.R., Jayakrishnan, A., Kumar, T.S., 2020. Combinational delivery of anticancer drugs for osteosarcoma treatment using electrosprayed core shell nanocarriers. J. Mater. Sci. Mater. Med. 31, 1–11.
Şahin, A., Eke, G., Buyuksungur, A., Hasirci, N., Hasirci, V., 2018. Nuclear targeting peptide-modified, DOX-loaded, PHBV nanoparticles enhance drug efficacy by targeting to Saos-2 cell nuclear membranes. J. Biomater. Sci. Polym. Ed. 29, 507–519.
Sarda, S., Iafisco, M., Pascaud-Mathieu, P., Adamiano, A., Montesi, M., Panseri, S., Marsan, O., Thouron, C., Dupret-Bories, A.s., Tampieri, A., 2018. Interaction of folic acid with nanocrystalline apatites and extension to methotrexate (antifolate) in view of anticancer applications. Langmuir 34, 12036–12048.
Shin, S.W., Song, I.H., Um, S.H., 2015. Role of physicochemical properties in nanoparticle toxicity. Nanomaterials 5, 1351–1365.
Steckiewicz, K.P., Barcinska, E., Sobczak, K., Tomczyk, E., Wojcik, M., Inkielewicz-Stępniak, I., 2020. Assessment of anti-tumor potential and safety of application of glutathione stabilized gold nanoparticles conjugated with chemotherapeutics. Int. J. Med. Sci. 17, 824.
Susa, M., Iyer, A.K., Ryu, K., Hornicek, F.J., Mankin, H., Amiji, M.M., Duan, Z., 2009. Doxorubicin loaded polymeric nanoparticulate delivery system to overcome drug resistance in osteosarcoma. BMC Canc. 9, 399.
Tapeinos, C., Battaglini, M., Prato, M., La Rosa, G., Scarpellini, A., Ciofani, G., 2018. CeO2 nanoparticles-loaded pH-responsive microparticles with antitumoral properties as therapeutic modulators for osteosarcoma. ACS Omega 3, 8952–8962.
Wang, L., Wang, W., Rui, Z., Zhou, D., 2016. The effective combination therapy against human osteosarcoma: doxorubicin plus curcumin co-encapsulated lipid-coated polymeric nanoparticulate drug delivery system. Drug Deliv. 23, 3200–3208.
Wei, H., Chen, J., Wang, S., Fu, F., Zhu, X., Wu, C., Liu, Z., Zhong, G., Lin, J., 2019. A nanodrug consisting of doxorubicin and exosome derived from mesenchymal stem cells for osteosarcoma treatment in vitro. Int. J. Nanomed. 14, 8603.
Wilczewska, A.Z., Niemirowicz, K., Markiewicz, K.H., Car, H., 2012. Nanoparticles as drug delivery systems. Pharmacol. Rep. 64, 1020–1037.
Yang, F., Wen, X., Ke, Q.-F., Xie, X.-T., Guo, Y.-P., 2018. pH-responsive mesoporous ZSM-5 zeolites/chitosan core-shell nanodisks loaded with doxorubicin against osteosarcoma. Mater. Sci. Eng. C 85, 142–153.
Yang, P., Zhang, L., Wang, T., Liu, Q., Wang, J., Wang, Y., Tu, Z., Lin, F., 2020. Doxorubicin and edelfosine combo-loaded lipid–polymer hybrid nanoparticles for synergistic anticancer effect against drug-resistant osteosarcoma. OncoTargets Ther. 13, 8055.
Zhang, B., Zhang, Y., Li, R., Li, J., Lu, X., Zhang, Y., 2020. The efficacy and safety comparison of first-line chemotherapeutic agents (high-dose methotrexate, doxorubicin, cisplatin, and ifosfamide) for osteosarcoma: a network meta-analysis. J. Orthop. Surg. Res. 15, 1–10.